CAMBRIDGE
UNIVERSITY PRESS

Regular Article

Neural effects of controllability as a key dimension of stress exposure

Emily M. Cohodes[1] , Paola Odriozola[1], Jeffrey D. Mandell[2], Camila Caballero[1], Sarah McCauley[1], Sadie J. Zacharek[1],
H. R. Hodges[1], Jason T. Haberman[1], Mackenzye Smith[1], Janeen Thomas[1], Olivia C. Meisner[1], Cameron T. Ellis[1],
Catherine A. Hartley[3] and Dylan G. Gee[1]

[1]Department of Psychology, Yale University, New Haven, CT, USA, [2]Program in Computational Biology and Bioinformatics, Yale University, New Haven, CT, USA
and [3]Department of Psychology, New York University, New York, NY, USA

Abstract

Cross-species evidence suggests that the ability to exert control over a stressor is a key dimension of stress exposure that may sensitize frontostriatal-amygdala circuitry to promote more adaptive responses to subsequent stressors. The present study examined neural correlates of stressor controllability in young adults. Participants ($N = 56$; $M_{age} = 23.74$, range = 18–30 years) completed either the controllable or uncontrollable stress condition of the first of two novel stressor controllability tasks during functional magnetic resonance imaging (fMRI) acquisition. Participants in the uncontrollable stress condition were yoked to age- and sex-matched participants in the controllable stress condition. All participants were subsequently exposed to uncontrollable stress in the second task, which is the focus of fMRI analyses reported here. A whole-brain searchlight classification analysis revealed that patterns of activity in the right dorsal anterior insula (dAI) during subsequent exposure to uncontrollable stress could be used to classify participants' initial exposure to either controllable or uncontrollable stress with a peak of 73% accuracy. Previous experience of exerting control over a stressor may change the computations performed within the right dAI during subsequent stress exposure, shedding further light on the neural underpinnings of stressor controllability.

Keywords: control; frontolimbic circuitry; stress reactivity; stress; stressor controllability

(Received 31 August 2021; revised 2 November 2021; accepted 2 November 2021)

Introduction

Decades of research on the pernicious effects of exposure to environmental adversity across the lifespan highlight a clear pathway from exposure to stressful contexts to increased risk for developing cognitive, social, emotional, and physical health problems (Boyce, 2007; Luthar, 1999; McLaughlin et al., 2010; McLoyd, 1998; Shonkoff et al., 2009, 2012). However, exposure to stress does not have a uniform effect for all individuals (Gabbay et al., 2004). Recent characterizations of the psychobiological effects of stress exposure have employed a dimensional approach, focused on how experiential, environmental, and timing-related factors may affect associations between stress exposure and functioning across multiple domains (Cohodes et al., 2020; Ellis et al., 2009; Fox et al., 2010; Gee & Casey, 2015; Manly et al., 2001; McLaughlin & Sheridan, 2016; Sheridan & McLaughlin, 2014; Tottenham & Sheridan, 2010). Clear delineation of these multilevel factors, which may moderate the impact of stress on neurodevelopment, development of psychopathology, and later functioning, is a critical step toward designing improved interventions that target an individual's neurodevelopmental stage and specific profile of past stress exposure to promote resilience.

Stressor controllability, or the degree to which an individual is able to exert control over an aversive experience by altering the intensity, duration, onset, or termination of the event, is one such factor that may moderate the behavioral and neurobiological impacts of stress. Experiences of control shape learning and behavioral development from a young age (Frankenhuis et al., 2013; Gunnar, 1980). Building on foundational research on learned helplessness that linked the ability to control biologically relevant stimuli in the environment with future behavior (Maier & Seligman, 1976), decades of animal research have demonstrated both short- and long-term benefits of exposure to controllable stress (Amat et al., 2010; Maier & Watkins, 2010; Seligman & Maier, 1967). Relative to animals exposed to uncontrollable stress, animals exposed to controllable stress exhibit more adaptive (i.e., active) coping responses to subsequent uncontrollable stress, both immediately and up to 1 week later (Amat et al., 2006, 2010), including when subsequent stress exposure is in another domain (Maier & Watkins, 2010). Translation of stressor controllability paradigms to human samples has shown that exposure to controllable stress modulates individuals' subsequent expression of cued or contextual conditioned fear. Relative to exposure to either an uncontrollable stress or a nonstressed control condition, fear is diminished following exposure to controllable stress (Hartley et al., 2014).

Counter to conventional notions of stress as universally harmful, the experience of controllable stress may inoculate an individual against negative effects of subsequent stress exposure by promoting long-term resilience and facilitating adaptive coping via increased plasticity in behavioral responding (Amat et al., 2010). Previous interactions with the environment likely inform

CrossMark

an individual's estimate of the likelihood that they will be able to control the environment (Ligneul et al., 2020) and therefore which behavioral strategies are likely to be most useful, "orchestrating a behavioral strategy that, according to historical experience, is most likely to be adaptive" (Moscarello & Hartley, 2017, p. 726). Individuals previously exposed to controllable stress may assume control and therefore enact adaptive coping strategies when presented with novel or uncertain environments, promoting resilience during subsequent exposure to uncontrollable stress. In line with this theory, recent experimental evidence demonstrated that prior exposure to controllable stress, as compared to uncontrollable stress, was associated with more exploratory behavior and reliance on a more active approach (i.e., more complex computations drawing upon available information about the environment) when estimating one's environmental control (Ligneul et al., 2020). These results highlight increased exploration and adaptive estimation of environmental control as a specific mechanism by which prior exposure to controllable stress may promote resilience during subsequent exposure to uncontrollable stress.

Although much remains unknown about the neural mechanisms underlying the effects of stressor controllability, evidence to date suggests that experiences of controllable stress modulate future responding to stress via alterations in corticolimbic circuitry. Exposure to controllable stress in rodents has been associated with increased serotonin release in the dorsal raphe nucleus (DRN) and blunted activation of the DRN via projections between the ventromedial prefrontal cortex (vmPFC) and inhibitory interneurons in the DRN, relative to uncontrollable stress (Baratta et al., 2009; Kubala et al., 2012). The DRN and vmPFC project directly to the amygdala, suggesting that exposure to controllable stress may engage projections that also serve to regulate amygdala reactivity to stress (Amat et al., 2006; Baratta & Maier, 2017; Liu et al., 2009).

In rodents, controllable stress may yield frontostriatal plasticity that enables subsequent stressors to more easily recruit the medial prefrontal cortex (mPFC; Mobbs & Kim, 2015), which may result in increased prefrontal regulation of the amygdala even when an individual does not have control over a subsequent stressor (Amat et al., 2008, 2010). Additionally, projections between the lateral nucleus, basal nucleus of the amygdala, and striatum are central to aversively motivated action in rodents. Direct, non-reciprocal projections between the basolateral amygdala and the ventral striatum transmit information about avoidance of the aversive stimulus that is critical for execution of the shuttling response (i.e., active avoidance of the aversive stimulus; Ramirez et al., 2015). Moreover, projections between the prelimbic cortex and ventral striatum may mediate avoidance and be central to observable effects of exposure to controllable stress (Bravo-Rivera et al., 2015). Taken together, these findings from the animal literature suggest that controllable stress may inoculate an individual against the harmful effects of subsequent exposure to stress through persistent modulation of neurocircuitry underlying stress reactivity (Amat et al., 2010).

Investigations of the neural mechanisms underlying these processes in humans are ongoing. Evidence to date suggests that, in human adults, the exertion of control over a stressor engages the ventral striatum, vmPFC, and lateral and basal nuclei of the amygdala, which promotes decreased stress reactivity and increased active coping behavior during exposure to subsequent stress (Boeke et al., 2017; Collins et al., 2014). Further, evidence suggests that an individual's ability to engage in active coping behaviors in order to successfully avoid a stressor is related to the functional synchronization between the ventral striatum,

vmPFC, and amygdala (Collins et al., 2014). Finally, adults who exhibited increased activation of the vmPFC during exposure to uncontrollable stress were found to be more persistent (Bhanji & Delgado, 2014), and reported using active coping strategies to a greater degree in their daily lives (Sinha et al., 2016), suggesting important translation of laboratory-based findings into real-world contexts.

The specific aim of the present study was to characterize how exposure to controllable stress (versus uncontrollable stress) impacts subsequent responding to uncontrollable stress. The current study presents neuroimaging findings for a pair of novel stressor controllability tasks in young adults, ages 18–30 years. During the first task, participants were exposed to either controllable or uncontrollable stress (between-subjects design). During the second task, all participants were exposed to uncontrollable stress. Building upon cross-species research on stressor controllability, we hypothesized that participants exposed to controllable stress—relative to their age- and sex-matched yoked counterparts exposed to uncontrollable stress—would show altered neural responding during subsequent exposure to uncontrollable stress. Specifically, we hypothesized that participants initially exposed to controllable stress would exhibit increased activation of the vmPFC, ventral striatum, and dorsal anterior cingulate cortex and reduced activation of the amygdala and superior temporal gyrus (due to its role in primary auditory sensory processing of aversive auditory stimuli; Zald & Pardo, 2002) during subsequent exposure to uncontrollable stress. Furthermore, we hypothesized that multivariate patterns could be used to reliably classify individuals based on prior experiences of control over a stressor during subsequent uncontrollable stress exposure. Specifically, multivariate patterns within the following brain regions theorized to be central to stressor controllability—ventral striatum, dorsal anterior cingulate cortex, superior temporal gyrus, amygdala, and vmPFC—were hypothesized to enable reliable classification of individuals' prior experiences of control.

Method

Participants

Fifty six adults completed the functional magnetic resonance imaging (fMRI) session (ages 18–30 years old, $M_{age} = 23.74$, $SD = 3.55$; 39 female, 17 male, no participants in sample reported nonbinary gender identity). Participants were recruited through community postings in New Haven, Connecticut. Participants were 45.5% Non-Hispanic White, ($n = 25$), 18.2% Asian ($n = 10$), 18.2% Black or African American ($n = 10$), 12.7% Hispanic/Latinx ($n = 7$), and 5.4% mixed or other race/ethnicity ($n = 3$). Information regarding race/ethnicity was missing for $n = 1$ participant. Participants had completed an average of 15.04 years of education ($SD = 2.26$). Participants were required to (a) be between the ages of 18–30; (b) be free of lifetime treatment with psychotropic medication; (c) have an IQ > 80; (d) be free of lifetime history of head trauma resulting in loss of consciousness for more than five minutes; (e) be right-handed; (f) be free of contraindication for magnetic resonance imaging (MRI) scanning; and (g) be free of chronic medical illness or neurological disorder. See Table 1 for full demographic information. In addition, participants were excluded if their in-scanner mean absolute translational or rotational motion in any of the 6 rigid directions was greater than 2 mm or 2°, respectively, if their mean relative (timepoint to timepoint) motion was greater than 0.2 mm, or if the percentage of data that would need to be regressed out due to motion outlier

Table 1. Demographic information

Participant demographic variables	$N = 56$
Age	
Mean ± SD	23.74 ± 3.55
Min–Max	18.74–30.92
Median (IQR)	23.32 (6.19)
Sex	
Male	17 (30.4%)
Female	39 (69.6%)
Race/ethnicity	
Non-Hispanic White	25 (45.5%)
Hispanic/Latino	7 (12.7%)
Black/African American	10 (18.2%)
Asian	10 (18.2%)
Other	1 (1.8%)
Mixed	2 (3.6%)
Years of education	
Mean ± SD	15.04 ± 2.26
Min–Max	12.00–20.00
Median (IQR)	16 (3.00)

timepoints in framewise displacement (FD; Power et al., 2012) exceeded 15% (see details in fMRI analyses section below).

Procedure

All participants identified as potentially eligible for the fMRI study provided written informed consent according to the procedures set forth and approved by the Institutional Review Board at Yale University. All participants completed a clinical interview at the first study visit to assess eligibility; eligible participants were invited for a 3-hr MRI scan visit during which they completed a simulated scan for motion training, questionnaires, and MRI scan procedures. At the scan visit, participants completed two stressor controllability tasks, further described below. For the first task, half of the participants were assigned to experience controllable stress, and half were assigned to experience uncontrollable stress. For the second task, all participants experienced uncontrollable stress.

Clinical assessment to determine eligibility

The Anxiety and Related Disorders Interview Schedule for DSM-5: Adult Version (ADIS-5; Brown & Barlow, 2014) was administered by trained research assistants and graduate students to assess for presence of current and past psychiatric disorders. Interviews were conducted during an in-person laboratory session and were supervised by a clinical psychologist. The Wechsler abbreviated scale of intelligence (Wechsler, 2011) was used to assess general intellectual functioning.

Prescan assessments and training

In order to familiarize participants with the scanner environment, all participants completed a 20-min mock scan session in a dedicated MRI simulator at the scanning facility (diameter of bore = 55–60 cm). Prior to completing scan procedures, participants completed motion training with behavioral shaping both with and without simultaneous completion of a practice task. During the

training session in the simulator, a modified Wii device was fitted to the participant's head with a strap in order to monitor motion and provide feedback to the participant in the form of a mild vibration whenever the participant exceeded a set motion threshold (protocol developed by Niles Oien at University of Colorado, Boulder; full description of motion compliance training is provided in the appendix of Heller, 2017). All motion training procedures paralleled those employed in the Adolescent Brain Cognitive Development Study (ABCD; Casey et al., 2018).

Following motion compliance training without simultaneous task performance, participants completed a behavioral task designed to simulate the motor demands of the two stressor controllability tasks while continuing to wear the Wii motion device and listening to prerecorded scanner noises. The practice behavioral task was a modified version of an open source Python-based game called the "Snowflake Game" (Kubierschky, 2009) that participants played with a replica of the response device used in the scanner in order to familiarize themselves with the button box (Trainer 4-Button Diamond-Pattern Button Box, Current Designs, Philadelphia, PA). Before proceeding with additional prescan setup procedures, all participants completed 90s of the practice task with zero motion events beyond an angle tolerance threshold of 2.

Stressor controllability fMRI tasks ("Balloon Game" and "Egg Game")

Task design

The novel developmentally adapted stressor controllability tasks used in the present study were loosely adapted from a previously validated task simulating stressor controllability in a laboratory setting (Hartley et al., 2014). The tasks were programmed in Python, with the use of the Psychopy package to implement graphics and user interaction features (Peirce, 2007). All graphics and auditory stimulus files were drawn from open sources and were publicly available for reuse. Although the current analyses focus on an adult sample, the tasks were carefully developed to optimize their use in child and adolescent samples to facilitate extension of stressor controllability research to human developmental samples in the future (i.e., tasks were designed to be optimally engaging for children and adolescents and all stimuli are developmentally appropriate).

Task versions. Participants completed two separate stressor controllability tasks (30 trials each) developed to present participants with a novel paradigm at both time points. The task developed for use at the first time point ("Balloon Game," henceforth referred to as "Task 1") is comprised of the controllable stress and uncontrollable stress conditions. The task developed for use at the second time point ("Egg Game," henceforth referred to as "Task 2") has only one condition—uncontrollable stress—that all participants complete. In Task 1 (see Figure 1 for depiction), during the *anticipatory period* (4 s), participants view a tree against a natural background (blue sky) framed in a yellow border. Next, during the *avoidance period* (4.5 s), the border changes to purple and a cluster of balloons floating toward the top of the screen appears. The balloons start at the bottom of the screen and move up in a variable, zigzagging pattern. Participants are presented with a hand in the bottom middle of the screen, which moves in response to each directional arrow key press (up, down, left, and right) made by the participant on a diamond-shaped button box that records behavioral responses (Trainer 4-Button Diamond-Pattern
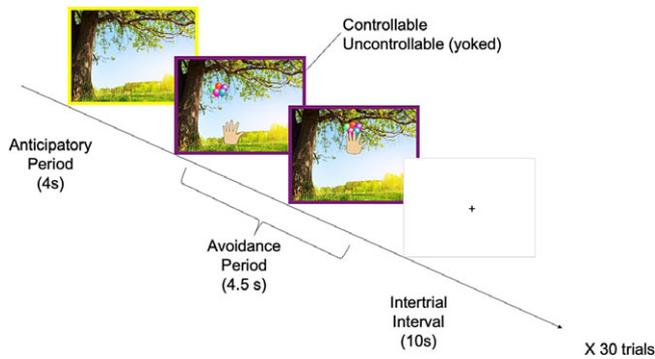
Figure 1. Task design of balloon game (Task 1). Task 1 consisted of 30 trials that began with participants viewing a tree against a natural background (blue sky) framed in a yellow border during the anticipatory period (4 s). Next, during the avoidance period (4.5 s), the border changed to purple and a cluster of balloons floating toward the top of the screen appeared. Participants were presented with a hand in the bottom middle of the screen, which moved in response to each directional arrow key press made by the participant. An intertrial interval consisting of a fixation cross (10 s) followed each trial. In the controllable stress condition, participants were exposed to an aversive popping noise associated with the balloon reaching the top of the screen at the conclusion of each trial if they did not intersect the hand with the balloon. If participants successfully intersected the balloon with the hand, the hand froze in the final position for the remainder of the trial. Participants in the uncontrollable stress condition were systematically exposed to the same stimuli as participants in the controllable stress condition and were able to move the arrow buttons to move the hand. These actions did not affect the reinforcement schedule; rather, the delivery of the aversive noise for participants in the uncontrollable stress condition was identical to that of their yoked controllable stress-exposed counterparts.

Figure 2. Task design of egg game (Task 2). Task 2 consisted of 30 trials that began with participants viewing an image of a counter with eggs on top, framed in a yellow border during the anticipatory period (4 s). Next, during the avoidance period (4.5 s), the border changed to purple and an egg began to fall from the counter in a random zigzag pattern. When the egg reached the bottom, it cracked on the ground (associated with an aversive cracking noise). Participants were presented with a hand in the top middle of the screen, and were able to explore various movements in the task environment in correspondence with button presses they made but, critically, these movements did not avert the aversive noise (i.e., all participants had no control over the aversive noise in this task). An intertrial interval consisting of a fixation cross (10 s) followed each trial.

Button Box, Current Designs, Philadelphia, PA). Participants are instructed to use the buttons to explore different actions during the trials, but are not explicitly instructed to try to "catch" the balloons with the hand. An intertrial interval consisting of a fixation cross (10 s) follows each trial.

In the controllable stress condition, participants were exposed to the aversive popping noise associated with the balloon reaching the top of the screen at the conclusion of each trial if they did not intersect the hand with the balloon as it ascended to the top of the screen. If participants successfully intersected the balloon with the hand, the hand froze in the final position for the remainder of the trial. Participants in the uncontrollable stress condition were age- and sex-matched to a participant in the controllable stress condition (i.e., "yoked"; Hartley et al., 2014). Same-sex participants were yoked within two years of age (mean difference between individuals in each yoked pair = 0.63 years, SD = 0.56, range = 0–2 years). Participants in the uncontrollable stress condition were systematically exposed to the same stimuli as participants in the controllable stress condition, were able to move the arrow buttons to move the hand, and were given the same instructions as their yoked counterparts in the controllable stress condition. These actions did not affect the reinforcement schedule; rather, the delivery of the aversive noise for participants in the uncontrollable stress condition was identical to that of their yoked controllable stress-exposed counterparts. The aversive noise in all conditions of both Task 1 and Task 2 was delivered at a volume ranging from 95 to 103 decibels for 500 ms, consistent with prior work (Meyer et al., 2019).

Following completion of Task 1, all participants completed a 7-min resting-state scan while viewing Inscapes (Vanderwal et al., 2015). Then, all participants completed Task 2 (see Figure 2 for depiction). Task 2 is identical in design to Task 1 but, rather than navigate the hand to intersect with a cluster of balloons, participants attempt to catch a series of eggs rolling off a counter before they
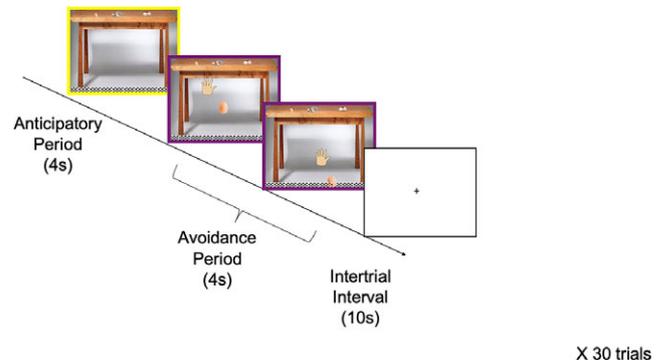
crack on the ground (associated with an aversive cracking noise). Like in Task 1, participants were able to explore various movements in the task environment in correspondence with various button presses on the button box (up, down, left, and right) but, critically, these movements did not avert the aversive noise.

Both Task 1 and Task 2 were divided into two parts (each segment of each task lasted 4 min and 53 s). Participants were instructed to take a 1-min break between the first and second parts of each task. Participants were fitted with a weighted blanket designed to reduce motion. All aversive stimuli were delivered via OptoAcoustics noise canceling headphones fitted to participants' ears for maximum reduction of external scanner noises (Kahana et al., 2004).

MRI

MRI acquisition parameters

Participants were scanned on one of two 3T Siemens Magnetom Prisma scanners (Siemens, Erlangen, Germany). N = 34 participants were scanned at the Magnetic Resonance Research Center and n = 22 participants were scanned at the Brain Imaging Center, both located at Yale University. All participants were scanned on the same scanner as their yoked counterpart. N = 46 participants were scanned with a 64-channel head coil using scan parameters based on nationwide neuroimaging data collection for the ABCD Study (Casey et al., 2018), and n = 10 participants were scanned with a 32-channel head coil. All participants were scanned using the same head coil as their yoked counterpart.

A whole-brain high-resolution T1-weighted anatomical scan magnetization-prepared rapid acquisition gradient echo (MPRAGE; 1070 ms TI, 2500 ms TR; 2.9 ms TE; 8° flip angle; 256 mm field of view (FoV); 176 slices in sagittal plane; 256 × 256 matrix; 2× parallel imaging; 1.0 × 1.0 × 1.0 mm resolution) was acquired for each participant for transformation, co-registration, and localization of functional data into Montreal Neurological Institute (MNI) space. A whole-brain high-resolution T2-weighted fast spin echo was also acquired for detection

and quantification of white matter lesions and cerebral spinal fluid (3200 ms TR; 565 ms TE; variable flip angle; 256 mm FoV; 176 slices in sagittal plane; 256 × 256 matrix; 2× parallel imaging; 1.0 × 1.0 × 1.0 mm resolution).

During each stressor controllability task, high spatial and temporal resolution multiband echo planar imaging (EPI) fMRI scans were collected with fast integrated distortion correction. A total of 60 axial slices covering the whole brain were imaged using a T2*-weighted EPI sequence (800 ms TR; 30 ms TE; 52° flip angle; 216 FoV; 90 × 90 matrix; 2.4 × 2.4 × 2.4 mm resolution; 6 multiband acceleration factor with interleaved acquisition). Congruent with Human Connectome Project (HCP) guidelines and to facilitate accurate spatial distortion correction, two spin echo EPI scans with opposite phase encoding directions were collected prior to each block of functional scans (Glasser et al., 2013).

fMRI preprocessing

Raw neuroimaging data were converted to Brain Imaging Data Structure (BIDS; Gorgolewski et al., 2016) using heudiconv (www.github.com/nipy/heudiconv) and preprocessed with the HCP minimal preprocessing pipeline (Glasser et al., 2013) using the BIDS apps (www.github.com/BIDS-Apps/HCPPipelines). The preprocessing of these data involved gradient distortion correction, EPI field map preprocessing and distortion correction, motion correction, nonlinear registration to the MNI template (MNI 152, 2 mm space), and grand-mean intensity normalization. Specifically, EPI fMRI images were corrected using spin echo EPI scans (see Glasser et al., 2013 for additional details on HCP minimal preprocessing pipeline). Data were then spatially smoothed using a full-width half-maximum 5 mm kernel in order to increase signal-to-noise ratio (Gardumi et al., 2016; Smith & Brady, 1997)

fMRI analyses
Individual-level analyses. Individual-level analyses were conducted using the Functional Magnetic Resonance Imaging of the Brain (FMRIB) Software Library (FSL, https://fsl.fmrib.ox.ac.uk/fsl). A whole-brain fMRI analysis was completed with Task 2 data using FSL version 5.11's FMRI Expert Analysis Tool (FEAT) version 6.00. In the lower-level FEAT analysis (Woolrich et al., 2001), predictors for each task condition (i.e., anticipatory period and avoidance period; see Figure 1) were convolved with a double-gamma canonical hemodynamic response function (HRF). Temporal derivatives of each predictor were added as confound terms to the general linear model (GLM) to account for slice-timing differences and variability in the HRF delay across regions. Timeseries were high-pass filtered with a cutoff of 90 s (estimated for our specific task design using FSL's *cutoffcalc* function) and pre-whitened within FMRIB's Improved Linear Model to correct for autocorrelations in the timeseries.

As in previous work from our group (Meyer et al., 2019), rigorous motion correction was implemented to limit the potential effects of motion on task-related results. Regressors for motion in each of the 6 rigid directions and their temporal derivatives, output from FSL's MCFLIRT (Jenkinson et al., 2002) during HCP minimal preprocessing, were added as nuisance regressors in each participant's lower-level design matrices. Additionally, FSL's *fsl_motion_outliers* function (https://fsl.fmrib.ox.ac.uk/fsl/fslwiki/FSLMotionOutliers) was used to detect timepoints that were corrupted by large motion in each participant's data. Specifically, outliers were defined using FD as the motion metric (Power et al., 2012) and the default definition of outliers (i.e., 1.5 times the interquartile range above the upper quartile;

Tukey, 1977). This function created a confound matrix with a regressor for every outlier timepoint detected that was added to the participant-specific lower-level design matrix to regress out the effect of these timepoints on the results. This approach is intended to address the effects of intermediate to large motion spikes– which corrupt images in such a way that linear motion parameter regression methods are unable to fix– without disrupting the temporal structure of the timeseries.

Whole-brain general linear model analyses. A higher-level analysis was conducted using fixed effects to create mean statistical images across the first and second runs of Task 2 for each participant. Finally, a group-level analysis in FEAT (Woolrich et al., 2004) was conducted using FMRIB's Local Analysis of Mixed Effects (FLAME 1 + 2) to compute the group differences for each contrast of interest in Task 2 (i.e., controllable vs. uncontrollable groups). This analysis was conducted using a paired-samples t-test such that the paired subjects were the yoked participants from Task 1. Final statistical images were thresholded in FEAT using a voxelwise threshold of $z > 3.1$ (i.e., two-tailed $p < .001$) and cluster p-threshold of $p < .05$, the FSL defaults.

Multivariate pattern analysis. A multivariate pattern analysis (MVPA; Kriegeskorte et al., 2006) was used to identify brain regions where spatial activation patterns between participants could be used to accurately classify participants into their corresponding condition assignment at Task 1 (i.e., participants who completed the controllable vs. uncontrollable stress conditions during Task 1) based on neural responses during subsequent exposure to stress (i.e., Task 2), during which all participants were exposed to uncontrollable stress.

Following the lower-level analysis from the whole-brain GLM, the t-statistic images (i.e., tstat) for the avoidance period for each participant for each of the two runs of Task 2 were concatenated into one image file containing 112 volumes (i.e., two volumes for each of n = 56 participants). The data were masked using the MNI 152 2 mm gray matter brain mask from MNITemplate (https://github.com/Jfortin1/MNITemplate) in order to reduce compute time and were then used as the input for the classifier. At each voxel v_i, a $3 \times 3 \times 3$ neighborhood searchlight centered at v_i was defined such that the spatial pattern in this neighborhood was a 27-dimensional vector. Support vector machine (SVM) classification was performed in python (python.org) using Brain Imaging Analysis Kit (BrainIAK) software (brainiak.org; Kumar et al., 2020) which draws on tools from sci-kit learn (Pedregosa et al., 2011). When training the linear SVM classifier, we used a soft-margin approach, setting the regularization parameter C equal to the default parameter of 1 in order to avoid overfitting the data. The number of iterations for the SVM was limited to 1,000 to accommodate compute time limitations.

At each voxel, a Leave-One-Out Cross-Validation procedure was used to measure the performance of the classifier in distinguishing individuals who had previously been assigned to the controllable versus the uncontrollable stress condition during the subsequent task. In order to train the classifier, data from one participant were left out at a time to be used as the "test set" while data from the remaining participants were used as the "training set." The class label estimated by the classifier on the test set was then compared against the true class (i.e., assignment to either controllable or uncontrollable stress exposure at Task 1). This process was repeated such that every participant was used once for testing purposes. The ratio of correctly estimated class labels to the total

number of observations, hereafter referred to as classification accuracy (CA), was then computed. The resulting 3D map of CA at every voxel was used to identify brain regions that distinguish the two groups during Task 2.

Permutation testing was used for significance testing. The labels (i.e., whether a participant was assigned to the controllable versus uncontrollable stress condition of Task 1) were randomly shuffled 1,000 times (while keeping both exemplars for each participant consistent in the randomization) and were subjected to a searchlight analysis conducted in the same manner as the original analysis. This generated a null distribution of CA scores that was unique to our dataset. CA values from the true analysis were then converted into p-values using this null distribution, such that for each voxel, we computed the rank of the true value compared to the values from the 1,000 permutations, resulting in a value between 0 and 1,000 for every voxel. Since we only had a priori hypotheses regarding high classification accuracies, a one-tailed test was used to convert the rank values to p-values for each voxel [p-value = ($n_{permutations}$ − rank) / $n_{permutations}$]. Significant CAs were determined using a one-tailed voxelwise threshold of $p < .05$. In order to compute cluster sizes to determine clusterwise p values, first, the true searchlight CA values were converted to z-scores using the mean and standard deviation of the CA for each voxel across the 1,000 permutations. Second, FSL's smoothest function was used to calculate the smoothness of the z-scored data. Lastly, the z-stat image was subjected to cluster inference using FSL's cluster function (https://fsl.fmrib.ox.ac.uk/fsl/fslwiki/Cluster) using Gaussian Random Field theory with a voxelwise threshold of $z = 1.65$ (corresponding to a p-value of .05 in a one-tailed test) and a cluster extent threshold of $p < .05$ (Hayasaka & Nichols, 2003). Clusters surviving both the voxelwise threshold and the clusterwise threshold were considered significant. All code used to conduct this MVPA is available on the Yale Clinical Affective Neuroscience and Development Lab's GitHub repository (https://github.com/Yale-CANDLab).

Results

Whole-brain general linear model analysis

We first examined differences in univariate fMRI responses during Task 2 between participants previously randomized to the controllable and uncontrollable stress conditions. No group differences in activation were detected at a voxelwise threshold of $p < .001$ and cluster threshold of $p < .05$.

MVPA

To further investigate differences in neural organization among participants previously exposed to controllable versus uncontrollable stress, we compared patterns of activation using an MVPA on fMRI data acquired during Task 2. This analysis highlighted one cortical region where activity patterns during Task 2 could be used to reliably classify whether a participant had been assigned to the controllable versus uncontrollable stress condition in the *prior* task (Task 1). High cross-validation CA values were found in a cluster in the right dorsal anterior insula (dAI) (peak CA = 73%, $p < .001$, cluster $p = .026$; MNI coordinates: 34, 22, 4) (Figure 3). Contrary to our hypotheses, no other regions were detected at a voxelwise threshold of $p < .05$ and cluster extent of $p < .05$.
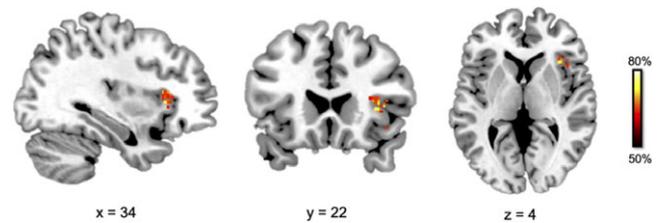

Figure 3. MVPA classifying previous exposure to controllable versus uncontrollable stress. Neural differences were found in the multivariate activation patterns associated with previous exposure to controllable versus uncontrollable stress in a cluster in the right dorsal anterior insula (dAI) (peak classification accuracy = 73%, $p > .001$, cluster $p = .026$; MNI coordinates: 34, 22, 4). Color bar (right) shows classification accuracy scores between 50% (about chance level) to 80%. These results indicate that a previous experience of control over a stressor may be associated with different computations in the dAI even during subsequent exposure to stress that is uncontrollable.

Discussion

The present study examined neural correlates of stressor controllability using a novel adaptation of a pair of stressor controllability tasks in a sample of adults. Building on the rich animal literature documenting increased adaptive responding to stress following exposure to controllable stress, as compared to uncontrollable stress (e.g., Maier & Watkins, 2005), and a growing body of human research (e.g., Boeke et al., 2017; Collins et al., 2014; Ligneul et al., 2020; Limbachia et al., 2021), the present study examined the neural correlates of the effect of previous exposure to controllable stress on subsequent responding to uncontrollable stress. We specifically aimed to isolate the effects of exertion of control over a stressor as a key dimension of stress exposure, while holding the timing, predictability, severity, and duration of the stressor constant.

Though no differences in univariate fMRI responses between participants previously assigned to the controllable and uncontrollable conditions were detected at the whole-brain level, results of the MVPA suggest that, even during universal experiences of uncontrollable stress, individuals previously exposed to controllable versus uncontrollable stress exhibited spatial activation patterns that were sufficiently distinct that they could be used to reliably discriminate an individual's past experience. Specifically, prior exposure to controllable versus uncontrollable stress was associated with reliably distinct patterns of activation of the right dAI during subsequent exposure to uncontrollable stress, suggesting that this may be an important neural signature of prior experiences of stressor controllability. These results indicate that previous experience of exerting control over a stressor has persistent effects on how the right dAI subsequently responds to uncontrollable stressors. Notably, this response is not related to an overall activation or deactivation, but rather a pattern of activity—reliably manifesting across participants—that characterizes the processing of exposure to new events characterized by uncontrollable stress.

As previous studies using both univariate and multivariate approaches have noted (Odriozola et al., 2016), this pattern may indicate that different types of computations are being performed in the right dAI based on participants' ability to exert control over a previously encountered stressor. This finding also points to the utility of multivariate approaches in detecting differences in brain activation patterns between distinct groups, beyond what may be revealed by employing only univariate analyses. Though the magnitude of dAI activation was not distinguishable between the controllable and uncontrollable stress-exposed groups, multivariate

findings highlight systematic differences in the neural computations performed by the dAI; thus, computations performed in this region during subsequent exposure to uncontrollable stress may not be reflected in simple differences in activation magnitude that are detectable by traditional univariate approaches.

Findings related to the right dAI were exploratory and underscore emerging understanding of the neurobiological underpinnings of stressor controllability as a key dimension of stress exposure. The anterior insula plays a central role in threat processing, particularly under conditions of uncertainty (Grupe & Nitschke, 2013; Paulus & Stein, 2006) and in threat and emotion processing more generally (Craig & Craig, 2009). Further, as a key node of the salience network, the dAI is implicated in detection of stimuli from the external world and in the coordination of dynamic neural resources necessary to respond to such stimuli (Uddin, 2015). In line with the present findings, the anterior insula may contribute to differential effects of controllable versus uncontrollable stress. Limbachia et al., (2021) found notable controllability-related decreases in anterior insula activation. Relatedly, relatively increased activation of the dAI during threat of unpredictable exposure to aversive stimuli has been found to be associated with low perceived control among anxious adults, further highlighting the insula as a region contributing to an individual's processing of anticipation of control in future events (Alvarez et al., 2015). Though we were unable to detect activation differences between the controllable and uncontrollable stress conditions using a univariate approach, we hypothesize that different multivariate patterns of anterior insula activation among participants exposed to controllable stress may be due to relatively diminished aversion or saliency prescribed to the stressor (i.e., the aversive noise) among controllable stress-exposed participants. Future studies are needed to further parse potentially varying roles of the insula in both anticipation of and actual exertion of control over aversive stimuli.

Despite a strong rationale for frontostriatal involvement in exposure to controllable versus uncontrollable stress, studies of the neurobiological underpinnings of the degree to which an individual is able to exert control over a stressor in humans have yielded a mixed pattern of findings. The lack of difference in vmPFC activation between groups reported in the current study is consistent with null findings in this region reported in Limbachia et al., (2021). Likewise, though the amygdala has been theorized to play a key role in modulation of avoidance learning (Moscarello & LeDoux, 2013), previous studies that have translated stressor controllability paradigms into human samples have also failed to detect differences in amygdala activation between controllable stress- and uncontrollable stress-exposed participants (Boeke et al., 2017). Future research in larger samples is needed to further examine the precise role of frontostriatal regions in modulating neurobiological responses to environments characterized by controllable versus uncontrollable stress.

Limitations and future directions

The present study had several limitations. First, the between-subjects conditions at Task 1 consisted of controllable stress and uncontrollable stress, without a no-stress control condition. Animal studies have elegantly demonstrated that exposure to controllable stress may have adaptive long-term effects on neurobehavioral outcomes, over and above exposure to no stress (see Maier & Watkins, 2010). Studies utilizing a triadic design including a no-stress condition are underway and will allow for more nuanced interpretation of the impacts of exposure to controllable versus uncontrollable stress. Critically, such studies will enable comparisons between exposure to each of these primary conditions and exposure to no stress at all, which could highlight the potential protective effects of exposure to controllable stress in humans.

Further, both stressor controllability tasks employed in the present study were administered during the same scanning session, precluding detection of longer-lasting effects of exposure to controllable stress and the potential neural mechanisms underlying a more durable effect. Future research should test the effects of controllable stress on neural engagement following a longer intertask interval to examine the durability and potency of these effects over time. Such research would continue to inform our understanding of potential conservation of the neural signatures of stressor controllability across animal and human studies and clarify the extent to which these effects may be useful for optimizing interventions to promote lasting resilience following stress. Lastly, as previously noted, though yoked pairs were matched on both scanner location and head coil, due to protocol changes mid-data collection, scans in the present study took place on two different scanners and utilized two different head coils.

A primary motivation for this broader line of research is that exposure to controllable stress may be particularly impactful prior to adulthood (Kubala et al., 2012), a period characterized by heightened sensitivity to stress (Blakemore & Mills, 2014; McLaughlin et al., 2015) and dynamic changes in the cortico-subcortical circuitry (Casey et al., 2019) thought to be relevant to stressor controllability. Rodent research suggests that exposure to controllable stress during the adolescent period mitigates the negative effects of uncontrollable stress exposure in adulthood (Kubala et al., 2012) by targeting the mPFC, blunting amygdala activation, and inhibiting behavioral responses during the subsequent stress exposure (Amat et al., 1998; Maier et al., 1993). These findings offer support for the potentially long-lasting effects of exposure to controllable stress (Kubala et al., 2012) and for the potential identification of periods during development when exposure to controllable stress may have particularly strong impacts on later functioning. Further, this line of work highlights the importance of future studies examining stressor controllability from a neurodevelopmental perspective in humans.

In conclusion, the present study adds to a growing body of literature examining the neural correlates of stressor controllability—a key dimension of stress exposure—and highlights the right dAI as a cortical region implicated in the response to controllable versus uncontrollable stress exposure. Here we show that previous exposure to controllable stress may alter the computations that are performed within the dAI during subsequent stress exposure. Though this line of research is in its infancy, to date, studies translating the rich animal literature on stressor controllability into human adult samples have collectively provided evidence that delineating the mechanisms underlying stressor controllability has the potential to inform novel interventions for individuals exposed to stress. Future research on the effects of controllable stress across development may inform the extent to which early experiences shape an individual's ability to leverage control over subsequent stressors as a potential buffer against exposure to uncontrollable stress.

References

Alvarez, R. P., Kirlic, N., Misaki, M., Bodurka, J., Rhudy, J. L., Paulus, M. P. . . . Drevets, W. C. (2015). Increased anterior insula activity in anxious individuals is linked to diminished perceived control. *Translational Psychiatry*, 5(6), e591–e591. https://doi.org/10.1038/tp.2015.84

Amat, J., Aleksejev, R. M., Paul, E., Watkins, L. R., & Maier, S. F. (2010). Behavioral control over shock blocks behavioral and neurochemical effects of later social defeat. *Neuroscience*, 165(4), 1031–1038. https://doi.org/10.1016/j.neuroscience.2009.11.005

Amat, J., Matus-Amat, P., Watkins, L. R., & Maier, S. F. (1998). Escapable and inescapable stress differentially alter extracellular levels of 5-HT in the basolateral amygdala of the rat. *Brain Research*, 812(1), 113–120. https://doi.org/10.1016/S0006-8993(98)00960-3

Amat, J., Paul, E., Watkins, L. R., & Maier, S. F. (2008). Activation of the ventral medial prefrontal cortex during an uncontrollable stressor reproduces both the immediate and long-term protective effects of behavioral control. *Neuroscience*, 154(4), 1178–1186. https://doi.org/10.1016/j.neuroscience.2008.04.005

Amat, J., Paul, E., Zarza, C., Watkins, L. R., & Maier, S. F. (2006). Previous experience with behavioral control over stress blocks the behavioral and dorsal raphe nucleus activating effects of later uncontrollable stress: Role of the ventral medial prefrontal cortex. *Journal of Neuroscience*, 26(51), 13264–13272. https://doi.org/10.1523/JNEUROSCI.3630-06.2006

Baratta, M. V., & Maier, S. F. (2017). New tools for understanding coping and resilience. *Neuroscience Letters*, 693, 54–57. https://doi.org/10.1016/j.neulet.2017.09.049

Baratta, M. V., Zarza, C. M., Gomez, D. M., Campeau, S., Watkins, L. R., & Maier, S. F. (2009). Selective activation of dorsal raphe nucleus-projecting neurons in the ventral medial prefrontal cortex by controllable stress. *European Journal of Neuroscience*, 30(6), 1111–1116. https://doi.org/10.1111/j.1460-9568.2009.06867.x

Bhanji, J. P., & Delgado, M. R. (2014). Perceived control influences neural responses to setbacks and promotes persistence. *Neuron*, 83(6), 1369–1375. https://doi.org/10.1016/j.neuron.2014.08.012

Blakemore, S.-J., & Mills, K. L. (2014). Is adolescence a sensitive period for sociocultural processing? *Annual Review of Psychology*, 65(1), 187–207. https://doi.org/10.1146/annurev-psych-010213-115202

Boeke, E. A., Moscarello, J. M., LeDoux, J. E., Phelps, E. A., & Hartley, C. A. (2017). Active avoidance: Neural mechanisms and attenuation of Pavlovian conditioned responding. *The Journal of Neuroscience*, 37(18), 4808–4818. https://doi.org/10.1523/JNEUROSCI.3261-16.2017

Boyce, W. T. (2007). A biology of misfortune: Stress reactivity, social context, and the ontogeny of psychopathology in early life. In A. S. Masten (Ed.),

Multilevel dynamics in developmental psychopathology: Pathways to the future (pp. 45–82). Taylor & Francis Group/Lawrence Erlbaum Associates.

Bravo-Rivera, C., Roman-Ortiz, C., Montesinos-Cartagena, M., & Quirk, G. J. (2015). Persistent active avoidance correlates with activity in prelimbic cortex and ventral striatum. *Frontiers in Behavioral Neuroscience*, 9, 184. https://doi.org/10.3389/fnbeh.2015.00184

Brown, T. A., & Barlow, D. H. (2014). *Anxiety and related disorders interview schedule for DSM-5 (ADIS-5L)*. Oxford University Press.

Casey, B. J., Cannonier, T., Conley, M. I., Cohen, A. O., Barch, D. M., Heitzeg, M. M. . . . Garavan, H. (2018). The adolescent brain cognitive development (ABCD) study: Imaging acquisition across 21 sites. *Developmental Cognitive Neuroscience*, 32, 43–54. https://doi.org/10.1016/j.dcn.2018.03.001

Casey, B. J., Heller, A. S., Gee, D. G., & Cohen, A. O. (2019). Development of the emotional brain. *Neuroscience Letters*, 693, 29–34. https://doi.org/10.1016/j.neulet.2017.11.055

Cohodes, E. M., Kitt, E. R., Baskin-Sommers, A., & Gee, D. G. (2020). Influences of early-life stress on frontolimbic circuitry: Harnessing a dimensional approach to elucidate the effects of heterogeneity in stress exposure. *Developmental Psychobiology*, 63(2), 153–172. https://doi.org/10.1002/dev.21969

Collins, K. A., Mendelsohn, A., Cain, C. K., & Schiller, D. (2014). Taking action in the face of threat: Neural synchronization predicts adaptive coping. *Journal of Neuroscience*, 34(44), 14733–14738. https://doi.org/10.1523/JNEUROSCI.2152-14.2014

Craig, A. D. (2009). How do you feel — now? The anterior insula and human awareness. *Nature Reviews Neuroscience*, 10(1), 59–70. https://doi.org/10.1038/nrn2555

Ellis, B. J., Figueredo, A. J., Brumbach, B. H., & Schlomer, G. L. (2009). Fundamental dimensions of environmental risk. *Human Nature*, 20(2), 204–268. https://doi.org/10.1007/s12110-009-9063-7

Fox, S. E., Levitt, P., & Nelson III, C. A. (2010). How the timing and quality of early experiences influence the development of brain architecture. *Child Development*, 81(1), 28–40. https://doi.org/10.1111/j.1467-8624.2009.01380.x

Frankenhuis, W. E., Gergely, G., & Watson, J. S. (2013). Infants may use contingency analysis to estimate environmental states: An evolutionary, life-history perspective. *Child Development Perspectives*, 7(2), 115–120. https://doi.org/10.1111/cdep.12024

Gabbay, V., Oatis, M. D., Silva, R. R., & Hirsch, G. (2004). Epidemiological aspects of PTSD in children and adolescents. In R. R. Silva (Ed.), *Posttraumatic stress disorder in children and adolescents: Handbook* (pp. 1–17, 1st ed.). WW Norton.

Gardumi, A., Ivanov, D., Hausfeld, L., Valente, G., Formisano, E., & Uludağ, K. (2016). The effect of spatial resolution on decoding accuracy in fMRI multivariate pattern analysis. *NeuroImage*, 132, 32–42. https://doi.org/10.1016/j.neuroimage.2016.02.033

Gee, D. G., & Casey, B. J. (2015). The impact of developmental timing for stress and recovery. *Neurobiology of Stress*, 1, 184–194. https://doi.org/10.1016/j.ynstr.2015.02.001

Glasser, M. F., Sotiropoulos, S. N., Wilson, J. A., Coalson, T. S., Fischl, B., Andersson, J. L. . . . Polimeni, J. R. (2013). The minimal preprocessing pipelines for the Human Connectome Project. *Neuroimage*, 80, 105–124. https://doi.org/10.1016/j.neuroimage.2013.04.127

Gorgolewski, K. J., Auer, T., Calhoun, V. D., Craddock, R. C., Das, S., Duff, E. P. . . . Halchenko, Y. O. (2016). The brain imaging data structure, a format for organizing and describing outputs of neuroimaging experiments. *Scientific Data*, 3, 160044. https://doi.org/10.1038/sdata.2016.44

Grupe, D. W., & Nitschke, J. B. (2013). Uncertainty and anticipation in anxiety: An integrated neurobiological and psychological perspective. *Nature Reviews Neuroscience*, 14(7), 488–501. https://doi.org/10.1038/nrn3524

Gunnar, M. R. (1980). Control, warning signals, and distress in infancy. *Developmental Psychology*, 16(4), 281. https://doi.org/10.1037/0012-1649.16.4.281

Hartley, C. A., Gorun, A., Reddan, M. C., Ramirez, F., & Phelps, E. A. (2014). Stressor controllability modulates fear extinction in humans. *Neurobiology of Learning and Memory*, 113, 149–156. https://doi.org/10.1016/j.nlm.2013.12.003

Hayasaka, S., & Nichols, T. E. (2003). Validating cluster size inference: Random field and permutation methods. *Neuroimage*, 20(4), 2343–2356. https://doi.org/10.1016/j.neuroimage.2003.08.003

Heller, S. C. Comparison of accuracy and movement for phonological grain size matching during fMRI scanning versus outside the scanner, 2017, (Doctoral dissertation, University of Colorado at Boulder).

Jenkinson, M., Bannister, P., Brady, M., & Smith, S. (2002). Improved optimization for the robust and accurate linear registration and motion correction of brain images. *Neuroimage*, 17(2), 825–841. https://doi.org/10.1016/s1053-8119(02)91132-8

Kahana, Y., Kots, A., Mican, S., Chambers, J., & Bullock, D.. *Optoacoustical ear defenders with active noise reduction in an MRI communication system.* Paper presented at the: INTER-NOISE and NOISE-CON Congress and Conference Proceedings, 2004, 1009–1024,

Kriegeskorte, N., Goebel, R., & Bandettini, P. (2006). Information-based functional brain mapping. *Proceedings of the National Academy of Sciences of the United States of America*, 103(10), 3863–3868. https://doi.org/10.1073/pnas.0600244103

Kubala, K. H., Christianson, J. P., Kaufman, R. D., Watkins, L. R., & Maier, S. F. (2012). Short-and long-term consequences of stressor controllability in adolescent rats. *Behavioural Brain Research*, 234(2), 278–284. https://doi.org/10.1016/j.bbr.2012.06.027

Kubierschky, M.. 'Snow Angel-1.1 2009, http://snowangel.knirz.de/snowangel-1.1.py

Kumar, M., Anderson, M., Antony, J., Baldassano, C., Brooks, P. P., Cai, M. B. . . . *et al.* (2020). *BrainIAK: The brain imaging analysis kit.* OSF Preprints, https://doi.org/10.31219/osf.io/db2ev,

Ligneul, R., Mainen, Z., Ly, V., & Cools, R. (2020). *Stress-sensitive brain computations of task controllability,* https://doi.org/10.1101/2020.11.19.390393

Limbachia, C., Morrow, K., Khibovska, A., Meyer, C., Padmala, S., & Pessoa, L. (2021). Controllability over stressor decreases responses in key threat-related brain areas. *Communications Biology*, 4(1), 1–11. https://doi.org/10.1038/s42003-020-01537-5

Liu, X., Tang, X., & Sanford, L. (2009). Stressor controllability and Fos expression in stress regulatory regions in mice. *Physiology & Behavior*, 97(3-4), 321–326. https://doi.org/10.1016/j.physbeh.2009.02.038

Luthar, S. S. (1999). *Poverty and children's adjustment.* Sage. https://doi.org/10.4135/9781452233758

Maier, S. F., Grahn, R. E., Kalman, B. A., Sutton, L. C., Wiertelak, E. P., & Watkins, L. R. (1993). The role of the amygdala and dorsal raphe nucleus in mediating the behavioral consequences of inescapable shock. *Behavioral Neuroscience*, 107(2), 377–388. https://doi.org/10.1037/0735-7044.107.2.377

Maier, S. F., & Seligman, M. E. (1976). Learned helplessness: Theory and evidence. *Journal of Experimental Psychology: General*, 105(1), 3. https://doi.org/10.1037/0096-3445.105.1.3

Maier, S. F., & Watkins, L. R. (2005). Stressor controllability and learned helplessness: The roles of the dorsal raphe nucleus, serotonin, and corticotropin-releasing factor. *Neuroscience & Biobehavioral Reviews*, 29(4-5), 829–841. https://doi.org/10.1016/j.neubiorev.2005.03.021

Maier, S. F., & Watkins, L. R. (2010). Role of the medial prefrontal cortex in coping and resilience. *Brain Research*, 1355, 52–60. https://doi.org/10.1016/j.brainres.2010.08.039

Manly, J. T., Kim, J. E., Rogosch, F. A., & Cicchetti, D. (2001). Dimensions of child maltreatment and children's adjustment: Contributions of developmental timing and subtype. *Development and Psychopathology*, 13(4), 759–782. https://doi.org/10.1017/S0954579401004023

McLaughlin, K. A., Green, J. G., Gruber, M. J., Sampson, N. A., Zaslavsky, A. M., & Kessler, R. C. (2010). Childhood adversities and adult psychopathology in the National Comorbidity Survey Replication (NCS-R) III: Associations with functional impairment related to DSM-IV disorders. *Psychological Medicine*, 40(5), 847–859. https://doi.org/10.1017/S0033291709991115

McLaughlin, K. A., & Sheridan, M. A. (2016). Beyond cumulative risk: A dimensional approach to childhood adversity. *Current Directions in Psychological Science*, 25(4), 239–245. https://doi.org/10.1177/0963721416655883

McLaughlin, K. A., Sheridan, M. A., Tibu, F., Fox, N. A., Zeanah, C. H., & Nelson, C. A. (2015). Causal effects of the early caregiving environment on development of stress response systems in children. *Proceedings of the National Academy of Sciences of the United States of America*, 112(18), 5637–5642. https://doi.org/10.1073/pnas.1423363112

McLoyd, V. C. (1998). Socioeconomic disadvantage and child development. *American Psychologist*, 53(2), 185. https://doi.org/10.1037//0003-066x.53.2.185

Meyer, H. C., Odriozola, P., Cohodes, E. M., Mandell, J. D., Li, A., Yang, R. . . . Liston, C. (2019). Ventral hippocampus interacts with prelimbic cortex during inhibition of threat response via learned safety in both mice and humans. *Proceedings of the National Academy of Sciences of the United States of America*, 116(52), 26970–26979. https://doi.org/10.1073/pnas.1910481116

Mobbs, D., & Kim, J. J. (2015). Neuroethological studies of fear, anxiety, and risky decision-making in rodents and humans. *Current Opinion in Behavioral Sciences*, 5, 8–15. https://doi.org/10.1016/j.cobeha.2015.06.005

Moscarello, J. M., & Hartley, C. A. (2017). Agency and the calibration of motivated behavior. *Trends in Cognitive Sciences*, 21(10), 725–735. https://doi.org/10.1016/j.tics.2017.06.008

Moscarello, J. M., & LeDoux, J. E. (2013). Active avoidance learning requires prefrontal suppression of amygdala-mediated defensive reactions. *Journal of Neuroscience*, 33(9), 3815–3823. https://doi.org/10.1523/JNEUROSCI.2596-12.2013

Odriozola, P., Uddin, L. Q., Lynch, C. J., Kochalka, J., Chen, T., & Menon, V. (2016). Insula response and connectivity during social and non-social attention in children with autism. *Social Cognitive and Affective Neuroscience*, 11(3), 433–444. https://doi.org/10.1093/scan/nsv126

Paulus, M. P., & Stein, M. B. (2006). An insular view of anxiety. *Biological Psychiatry*, 60(4), 383–387. https://doi.org/10.1016/j.biopsych.2006.03.042

Pedregosa, F., Varoquaux, G., Gramfort, A., Michel, V., Thirion, B., Grisel, O. . . . Duchesnay, É. (2011). Scikit-learn: Machine learning in Python. *Journal of Machine Learning Research*, 12(85), 2825–2830.

Peirce, J. W. (2007). PsychoPy—Psychophysics software in Python. *Journal of Neuroscience Methods*, 162(1-2), 8–13. https://doi.org/10.1016/j.jneumeth.2006.11.017

Power, J. D., Barnes, K. A., Snyder, A. Z., Schlaggar, B. L., & Petersen, S. E. (2012). Spurious but systematic correlations in functional connectivity MRI networks arise from subject motion. *Neuroimage*, 59(3), 2142–2154. https://doi.org/10.1016/j.neuroimage.2011.10.018

Ramirez, F., Moscarello, J. M., LeDoux, J. E., & Sears, R. M. (2015). Active avoidance requires a serial basal amygdala to nucleus accumbens shell circuit. *Journal of Neuroscience*, 35(8), 3470–3477. https://doi.org/10.1523/JNEUROSCI.1331-14.2015

Seligman, M. E., & Maier, S. F. (1967). Failure to escape traumatic shock. *Journal of Experimental Psychology*, 74(1), 1–9. https://doi.org/10.1037/h0024514

Sheridan, M. A., & McLaughlin, K. A. (2014). Dimensions of early experience and neural development: Deprivation and threat. *Trends in Cognitive Sciences*, 18(11), 580–585. https://doi.org/10.1016/j.tics.2014.09.001

Shonkoff, J. P., Boyce, W. T., & McEwen, B. S. (2009). Neuroscience, molecular biology, and the childhood roots of health disparities: Building a new framework for health promotion and disease prevention. *Journal of the American Medical Association*, 301(21), 2252–2259. https://doi.org/10.1001/jama.2009.754

Shonkoff, J. P., The Committee on Psychosocial Aspects of Child and Family Health, Committee on Early Childhood Adoption, and Dependent Care, and Section on Developmental and Behavioral Pediatrics, Siegel, B. S., Dobbins, M. I., Earls, M. F., Garner, A. S. . . . Wood, D. L. (2012). The lifelong effects of early childhood adversity and toxic stress. *Pediatrics*, 129(1), e232–e246, https://doi.org/10.1542/peds.2011-2663

Sinha, R., Lacadie, C. M., Constable, R. T., & Seo, D. (2016). Dynamic neural activity during stress signals resilient coping. *Proceedings of the National Academy of Sciences of the United States of America*, 113(31), 8837–8842. https://doi.org/10.1073/pnas.1600965113

Smith, S. M., & Brady, J. M. (1997). SUSAN—A new approach to low level image processing. *International Journal of Computer Vision*, 23(1), 45–78. https://doi.org/10.1023/A:1007963824710

Tottenham, N., & Sheridan, M. A. (2010). A review of adversity, the amygdala and the hippocampus: A consideration of developmental timing. *Frontiers in Human Neuroscience*, 3, 68. https://doi.org/10.3389/neuro.09.068.2009

Tukey, J. W. (1977). *Exploratory data analysis.* Addison-Wesley.

Uddin, L. Q. (2015). Salience processing and insular cortical function and dysfunction. *Nature Reviews Neuroscience*, *16*(1), 55–61. https://doi.org/10.1038/nrn3857

Vanderwal, T., Kelly, C., Eilbott, J., Mayes, L. C., & Castellanos, F. X. (2015). Inscapes: A movie paradigm to improve compliance in functional magnetic resonance imaging. *Neuroimage*, *122*, 222–232. https://doi.org/10.1016/j.neuroimage.2015.07.069

Wechsler, D. (2011). *Wechsler abbreviated scale of intelligence, Second edition (WASI-II).* NCS Pearson.

Woolrich, M. W., Behrens, T. E., Beckmann, C. F., Jenkinson, M., & Smith, S. M. (2004). Multilevel linear modelling for FMRI group analysis using Bayesian inference. *Neuroimage*, *21*(4), 1732–1747. https://doi.org/10.1016/j.neuroimage.2003.12.023

Woolrich, M. W., Ripley, B. D., Brady, M., & Smith, S. M. (2001). Temporal autocorrelation in univariate linear modeling of FMRI data. *NeuroImage*, *14*(6), 1370–1386. https://doi.org/10.1006/nimg.2001.0931

Zald, D. H., & Pardo, J. V. (2002). The neural correlates of aversive auditory stimulation. *NeuroImage*, *16*(3, Part A), 746–753. https://doi.org/10.1006/nimg.2002.1115